

Novel Backoff Mechanism for Mitigation of Congestion in DSRC Broadcast

Seungmo Kim, *Member, IEEE*, and Byung-Jun Kim

Abstract—Due to the recent re-allocation of the 5.9 GHz band by the US Federal Communications Commission (FCC), it will be inevitable that dedicated short-range communications (DSRC) and cellular vehicle-to-everything (C-V2X), two representative technologies for V2X, have to address coexistence. Especially, the distributed nature of DSRC makes it not trivial to control congestions, which makes it inefficient to disseminate a controlling signal. To this end, we propose a method to “lighten” a distributed V2X networking. Technically, it is to allocate the backoff counter according to the level of an accident risk to which a vehicle is temporarily exposed. We provide an analysis framework based on a spatiotemporal analysis. The numerical results show the improvement in the successful delivery of basic safety messages (BSMs).

Index Terms—V2X, 5.9 GHz, DSRC, CSMA, Backoff

I. INTRODUCTION

1) *Background on the 5.9 GHz Band:* In 1999, the US Federal Communications Commission (FCC) allocated the 5.9 GHz band for intelligent transportation system (ITS) applications based on dedicated short-range communications (DSRC) and adopted basic technical rules for the DSRC operations [1]. The DSRC is now at the stake of sharing the 5.9 GHz band with other radio technologies (RATs).

The first RAT is Wi-Fi. As suggested by the Congress in September 2015, the FCC, in its latest public notice [2], now seeks to refresh the record of its pending 5.9 GHz rulemaking to provide potential sharing solutions between proposed Unlicensed National Information Infrastructure (U-NII) devices and DSRC operations in the 5.9 GHz band. The current focus of the FCC’s solicitation in [2] is two-fold: (i) prototype of interference-avoiding devices for testing; (ii) test plans to evaluate electromagnetic compatibility of unlicensed devices and DSRC.

More recently, the cellular vehicle-to-everything communications (C-V2X) is seeking to operate in the 5.9 GHz band as well [3]. At present, only DSRC is permitted to operate in the ITS band in US, while the 5G Automotive Association (5GAA) has requested a waiver to the FCC to allow C-V2X operations in the band [3]. The key problem here is that C-V2X and DSRC are not compatible with each other. It means that if some vehicles use DSRC and others use C-V2X, these vehicles will be unable to communicate with each other—a scenario where the true potential of V2X communications cannot be attained.

S. Kim is with Department of Electrical and Computer Engineering, Georgia Southern University in Statesboro, GA, USA (e-mail: seungmokim@georgiasouthern.edu). B. J. Kim is with Department of Statistics at Virginia Tech in Blacksburg, VA, USA (e-mail: bjkim702@vt.edu).

2) *Significance of DSRC:* Nevertheless, DSRC still holds significance as the key technology enabling safety-critical applications [4]. Europe recently mandated DSRC as the sole technology operating in the 5.9 GHz band [5]. Also, in the US, 50 state transport departments request reserving the 5.9 GHz band for transport safety [6]. However, state departments of transportation (DOTs) are experiencing confusion and inefficiency in enhancement/expansion of connected vehicle technologies, due to the FCC’s indecisiveness on “shared use” of the 5.9 GHz band with other wireless systems i.e., Wi-Fi and C-V2X [6]. Also, at the US DOT, Phase I of a three-phase testing plan has been completed, which investigated the DSRCs interoperability with the other wireless systems [7]. However, Phase II has not yet even started, which is supposed to involve basic field tests to assess the efficacy of findings from Phase I [8]. Until these real-world tests are completed, one will not know conclusively to what extent, or whether at all, DSRC and the other technologies can operate together without interference, which has significant influence on the vehicle safety and mobility.

3) *Need for Lightening Load in DSRC:* A key requirement of V2V communication is the reliable delivery of safety messages. However, it has been found that a DSRC network can be congested even in simple traffic scenarios due to the limited bandwidth [9]. In addition, the FCC reduced the bandwidth for DSRC from 75 MHz to 10 MHz under possible coexistence with C-V2X [10]. As has been found from previous studies [11]–[17], it is not a trivial problem to achieve coexistence among dissimilar RATs not being able to coordinate with each other.

Relevant proposals modeled the crash risk and used it in enhancement of multiple access in V2X networks [18][19]. Another method is the enhanced distributed channel access (EDCA). However, the complicated backoff model [20] is not practical in the delay-constrained nature of a V2X safety-critical network. According to a latest study [21], the classical DSRC backoff model based on the distributed coordinated function (DCF) already yielded quite low probabilities of transmission within a beaconing period.

Motivated from the limitations of the currently available methods, this paper proposes a multiple access scheme that can be applied to a decentralized V2X network and can be performed at each vehicle without external support from infrastructure—e.g., roadside units (RSUs). The contributions of this paper are summarized as

- First, it defines a formula of a crash risk as a function of the variance of a vehicle’s speed from the neighboring vehicles.

- Second, this paper proposes a novel backoff allocation mechanism for DSRC, based on the crash risk. The mechanism features direct compatibility to the currently operated *distributed* V2X networking standards—e.g., DSRC and C-V2X mode 3—due to its simple applicability, which shall be elaborated in Section IV. The distributed nature is worth being kept because of the potential in a wide variety of applications—e.g., blockchain [22].
- It describes a carrier-sense multiple access (CSMA) using a more precise Markov chain taking into account a *packet expiration*, which is idiosyncratically critical to DSRC unlike other IEEE 802.11-based technologies. In fact, our results show that a DSRC network is more constrained by an expiration rather than a collision over the air. The CSMA has a key benefit: once programmed, the protocol can be executed at each vehicle without any scheduling from the infrastructure.
- In addition to the widely accepted classical metrics for providing easy understanding for audience, we also evaluate the proposed protocol based on inter-reception time (IRT) as a metric that adds further perspectives in analysis.

II. RELATED WORK

A. Markov Chain Model for IEEE 802.11p MAC

Carrier sense multiple access with collision avoidance (CSMA/CA) for the general IEEE 802.11 has been modeled as a two-dimensional Markov chain [23]. However, in DSRC, the contention window size does not get doubled even upon a packet collision, which simplifies the Markov chain structure.

The key difference in our model is that for BSM broadcast in a DSRC system, the probability of decrementing a backoff counter is not 1. Also, a Markov chain has been proposed to model on the broadcast of safety messages in DSRC [24]; yet it does not take into account a packet expiration (EXP) during a backoff process. Further, there was another aspect about which the model did not describe completely accurately. According to the IEEE 802.11p-2010 standard [25], the fundamental access method of the IEEE 802.11 medium access control (MAC) is a distributed coordination function (DCF), which shall be implemented in all stations (STAs). Investigating the CSMA/CA written in IEEE 802.11 MAC [23][26], the probability of transmission at the state of backoff being 0 still requires the probability of $1 - P_b$ for a transmission (where P_b denotes the probability of a slot being busy).

Also, the previous models suggested for analyzing the 802.11p beaconing have paid little attention to the varying number of contending nodes [27] and the restricted channel access of the control channel (CCH), i.e., Channel 178 (5.885-5.895 GHz) [28]. Since the 802.11p MAC protocol is a contention-based scheme, the joint effect of the varying number of contending nodes and the restricted channel access may lead the network to perform quite differently [29].

Given the significance of an EXP in determining the performance of a DSRC system, the models cannot be considered to completely accurately characterize the behavior of a safety message broadcast. In this work, we develop a new mathematic model that integrates those two factors.

B. Performance Metric

Motivated from limitations of classical metrics such as packet delivery rate (PDR) and latency, various other metrics have been proposed in the literature. The *inter-reception time (IRT)* is a superior metric in the sense that it is able to display both successful and failed transmissions at once. A latest work proposed an algorithm that adapts the frequency of BSM broadcast according to the IRT [30]. When IRT becomes to exceed a threshold, the frequency of transmission is decremented. The decrement goes until it reaches the minimum. While this work tackles a significant problem of managing the IRT, which much previous work overlooks while relying only on classical metrics such as PDR and latency, it does not provide enough mathematical and analytical detail on how exactly formulate the IRT. The same limitation is observed from other simulation-based work [31][32][33][34][35] and experiment-based work [36][37].

Besides the aforementioned metrics, some other metrics have also been used to evaluate the performance of congestion control techniques. Examples include the probability of successful reception of beacon message [38], update delay [39] as the elapsed time between two consecutive BSMs successfully received from the same transmitter, a 95% Euclidean cut-off error (in meters) [40], and information dissemination rate (IDR) [41].

C. DSRC Performance Enhancement Scheme

1) *EDCA*: There is body of work enhancing the performance of DSRC based on EDCA [43]. However, we remind that this paper particularly aims to enhance the performance of DSRC broadcast by prioritizing vehicles at high crash risks. We consider that the EDCA is not enough to achieve that purpose. First, increasing the load of real time data traffic will increase the collision in the network. Thus, delay time and packet loss percentage will increase more than the requirements of quality of service (QoS) [44]. Second, EDCA is known to be susceptible to additional load [45], which makes inadequate for a dynamic, distributed V2X network. Third, EDCA has been found not be able to support fairness when STAs in a network require diverse QoS requirements [46]. Fourth, as shall be presented in Section VI, a DSRC network is “contention-constrained” rather than collision-constrained due to the backoff process for CSMA. It yields an inefficiency of a too large CW, which in turn causes a very high probability of EXP. On the other hand, a too small CW can cause a collision, but it is rare in DSRC due to a large number of slots within a beaconing period—i.e., 1500 slots with 100 msec of inter-broadcast interval (IBI) and 66.7 μ sec of a slot time [42]. Considering the significance of safety-critical applications (indeed far more significant than delivering “voice” messages at a higher data rate), a more aggressive approach is needed to guarantee prioritization of vehicles with higher crash risk levels;

2) *Protocol Independent of CW*: Elaborating the last point, our desire is to design a protocol that optimizes a DSRC network regardless of CW. In the current 802.11 MAC mechanism, the CW size is dictated to take discrete values from a

bounded finite set [47]. The limitations of this constraint have been investigated [48], to discover that the limitation on the CW size in the main bottleneck in a dense network. Also, the BEB scheme has been found not to provide adequate level of fairness due to little correlation between a backoff time and a CW [49]. Furthermore, the IEEE 802.11 BEB backoff time calculation adjusts extremely rapidly [50]; the node backs off quickly when a collision is detected and also reduces its backoff time to CW_{min} immediately upon a successful transmission. This produces a large variation in the backoff time; every new packet after a successful delivery starts with CW_{min}, which may be too small for a heavy network load. It can easily lead to a higher level of network congestion. For these reasons, application of the current BEB that heavily relies on adaptation of CW has been found inefficient for distributed networks [51].

3) *Inter-RAT Coexistence in the 5.9 GHz Band*: The coexistence problem among dissimilar RATs in the 5.9 GHz band has been discussed in the literature: (i) between DSRC and Wi-Fi [52] and (ii) between DSRC and Wi-Fi/C-V2X [21].

Modification of CSMA was proposed for relieving bandwidth contention among vehicles within an IEEE 802.11p network [53]. The inter-vehicle distance was selected as the factor representing the risk of a crash. A message prioritization scheme among different classes of vehicles was proposed for military vehicles over commercial ones [18]. The key limitation was a relatively simple model for the stochastic geometry: a single junction of two 6-lane road segments. Such an urban model may lose generality when applied to other scenarios.

In another latest work, a reinforcement learning-based approach was proposed to address the dynamicity of a V2X networking environment [54]. Each vehicle needs to recognize the frequent changes of the surroundings and apply them to its networking behavior, which was formulated as a multi-armed bandit (MAB) problem. The MAB-based reinforcement learning enabled a vehicle, without any assistance from external infrastructure, to (i) learn the environment, (ii) quantify the accident risk, and (iii) adapt its backoff counter according to the risk.

III. SYSTEM MODEL

For formulation of the DSRC broadcast performance, this paper establishes the following key assumptions.

Assumption 1 (Node Distribution as PPP). A *generalized “square” space is assumed instead of an example road segment, for the most generic form of analysis as done in a related literature [22]. The environment represented by the system space \mathbb{R}_{sys}^2 , which is defined on a rectangular coordinate with the width and length of D m. Therein, a DSRC network is defined as a homogeneous Poisson point process (PPP), denoted by Φ_D , with the density of $\lambda (> 0)$. The position of vehicle i is denoted by $\mathbf{x}_i = (x_i, y_i) \in \mathbb{R}_{sys}^2$. Note also that the PPP discussed in this paper is a stationary point process where the density λ remains constant according to different points in \mathbb{R}_{sys}^2 .*

It is important to note that based on the modeling with PPP, the uniformity property of a homogeneous point process can be held [56]. That is, if a homogeneous point process is defined on a real linear space, then it has the characteristic that the positions of these occurrences on the real line are uniformly distributed. Therefore, we can assume that the DSRC vehicles are uniformly randomly scattered on the road with different values of intensities and CW values, which will be provided in Section VI.

Assumption 2 (Four Types of Packet Transmission Result). *There are four possible results of a packet transmission including successful delivery (SUC) and two types of collision: synchronized transmission (SYNC) and hidden-node collision (HN) [55]. A SUC is a case where a packet does not undergo contention nor collision. A SYNC refers to a situation where more than one Tx’s start transmission at the same time. A HN is the other type of collision, which occurs due to a hidden node.*

Assumption 3 (Consideration of BSM Broadcast in CCH). *The analysis framework and result that will be presented throughout this paper are based on assumption of using the CCH only—i.e., channel 178 in the 5.9 GHz band. It means that the result has a room for improvement if the network’s channel selection is expanded among the other shared channels (SCHs). As such, the results that will be demonstrated in Section VI can be regarded as the worst-case, most conservative ones.*

Assumption 4 (Speed as the Representative Factor of Crash Risk). *Speed has been found as the most direct indicator of a crash risk [59]. This paper assumes that each vehicle moves at speed of v meters per second (m/s), which is a varied factor as shall be shown in Section VI. The direction of a vehicle follows a uniform distribution in the range of $[0, 2\pi]$. A node is bounced off when reaching at the end of \mathbb{R}^2 in order to stay in the space, which hence keeps the total intensity the same.*

Remark 1 (Distribution of vehicle speed). *Speeds are selected by the driver. Different drivers select different speeds, dependent upon many variables (vehicle limitations, roadway conditions, driver ability, etc.). No single speed value can accurately represent all the speeds at a certain location. A speed distribution provides that information. Operating speeds have been found to be normally distributed [58]. This is fortunate since using that premise (probability is normally distributed) allows for some straightforward calculations.*

Definition 1 (Variance of speed: crash risk measurement metric). *We use the variance of speed from the speed limit of the road as the metric measuring the risk of a crash. The rationale behind this is the “easiness” in getting a speed limit. For instance, a speed limit is an easy number to obtain in many commercial GPS applications (e.g., Google Maps). Reliance on such an easily available quantity increases the applicability of the proposed algorithm. It can be replaced*

with other relevant parameters: e.g., the mean speed over the neighboring vehicles.

$$\Psi = \sqrt{(v - v_L)^2} \quad (1)$$

where v_L gives the speed limit of the road.

Definition 2 (Marked point process). *The PPP Φ is defined as a “marked” point process where the speed variance, Ψ , is associated with each point \mathbf{x}_i . This mark is an independent normal random variable as seen from a point \mathbf{x}_i . Specifically, let point process $\Phi = \{\mathbf{x}_i; i \in \mathbb{N}\}$ denote the locations of the nodes.*

Importantly, it is assumed that the mark of a point does not depend on the location of its corresponding point in the underlying (state) space.

IV. PROPOSED PROTOCOL

As have already mentioned in Section III, we choose the variation of speed, denoted by Ψ , as the key indicator of a crash risk to a vehicle is exposed while driving. As such, the proposed protocol allocates the backoff counter according to the quantity of Ψ .

We wanted a more aggressive scheme to benefit “dangerous” vehicles than allocating a higher access category (AC) in EDCA. In essence, the performance of EDCA still depends on CW, which may be hazardous for a very urgent safety-related packet delivery.

We remind that the key metric in the proposed protocol is Ψ that was presented in Proposition 1. The main idea of the proposed protocol is to divide the distribution of Ψ into multiple *discrete sections* and apply different *backoff allocation patterns*.

As such, we start with formulating the distribution of Ψ . We find the probability distribution function (PDF) as in the following Lemma:

Lemma 1 (Distribution of Ψ). *As shown in Fig. 1, the speed’s variance, Ψ , is found to follow the following distribution:*

$$f_{\Psi}(\psi) = \frac{1}{\sqrt{2\pi}\sigma} \psi^{-\frac{1}{2}} e^{-\frac{\psi}{2\sigma^2}}, \quad \psi \geq 0 \quad (2)$$

Proof: Let random variable Ψ be defined as $\Psi = (X - \mu)^2$ where $X \sim \mathcal{N}(\mu, \sigma^2)$.

For $\psi < 0$, since Ψ cannot have a negative value,

$$\mathbb{P}(\Psi < \psi) = 0 \quad (3)$$

For $\psi \geq 0$,

$$\begin{aligned} \mathbb{P}(\Psi < \psi) &= \mathbb{P}\left((X - \mu)^2 < \psi\right) \\ &= \mathbb{P}\left(-\sqrt{\psi} < X - \mu < \sqrt{\psi}\right) \\ &= \mathbb{P}\left(-\sqrt{\psi} + \mu < X < \sqrt{\psi} + \mu\right) \\ &= F_X\left(\mu + \sqrt{\psi}\right) - F_X\left(\mu - \sqrt{\psi}\right) \end{aligned} \quad (4)$$

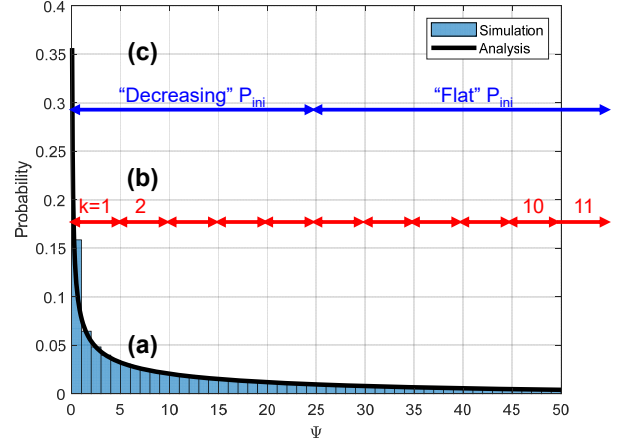


Fig. 1: PDF of Ψ (with $X \sim \mathcal{N}(60, 25)$): (a) Model validation between simulation and analysis of $f_S(s)$; (b) Categorization of Ψ (with $K = 11$ and $Q = 5$); and (c) An example allocation of backoff values for the proposed protocol (division of “decreasing” and “flat” at $k = \lfloor K/2 \rfloor$)

Therefore,

$$\begin{aligned} f_{\Psi}(\psi) &= \frac{d}{d\psi} \left[F_X(\mu + \sqrt{\psi}) - F_X(\mu - \sqrt{\psi}) \right] \\ &= \frac{d}{d\psi} \left[\int_{-\infty}^{\mu + \sqrt{\psi}} \frac{1}{\sqrt{2\pi}\sigma} e^{-\frac{(t-\mu)^2}{2\sigma^2}} dt \right. \\ &\quad \left. - \int_{-\infty}^{\mu - \sqrt{\psi}} \frac{1}{\sqrt{2\pi}\sigma} e^{-\frac{(t-\mu)^2}{2\sigma^2}} dt \right] \\ &= \frac{1}{\sqrt{2\pi}\sigma} \frac{d}{d\psi} \left[\int_{-\infty}^{\mu + \sqrt{\psi}} e^{-\frac{(t-\mu)^2}{2\sigma^2}} dt - \int_{-\infty}^{\mu - \sqrt{\psi}} e^{-\frac{(t-\mu)^2}{2\sigma^2}} dt \right] \\ &= \frac{1}{\sqrt{2\pi}\sigma} \left[e^{-\frac{\psi}{2\sigma^2}} \frac{d}{d\psi} (\mu + \sqrt{\psi}) - e^{-\frac{\psi}{2\sigma^2}} \frac{d}{d\psi} (\mu - \sqrt{\psi}) \right] \\ &= \frac{1}{\sqrt{2\pi}\sigma} \left[e^{-\frac{\psi}{2\sigma^2}} \frac{1}{2} \psi^{-\frac{1}{2}} + e^{-\frac{\psi}{2\sigma^2}} \frac{1}{2} \psi^{-\frac{1}{2}} \right] \\ &= \frac{1}{\sqrt{2\pi}\sigma} \psi^{-\frac{1}{2}} e^{-\frac{\psi}{2\sigma^2}} \end{aligned} \quad (5)$$

which completes the proof. \blacksquare

To represent the crash risk, we categorize the metric, Ψ , into a number of regions on its PDF. The reason for this categorization is, as seen from Fig. 1, the PDF of Ψ is open-ended to the right (positive side); hence, a value of Ψ itself is not appropriate to be used in categorization.

Proposition 1 (Categorization of Ψ). *Note that two key parameters are defined to identify a categorization: (i) the number of categories, K , and (ii) the step size, Q . The range of Ψ for each category, k , is given by*

$$(k-1)Q + 1 \leq \Psi \leq kQ, \quad (6)$$

which, in turn, gives k as a function of Ψ as

$$k = f(\Psi) = \left\lceil \frac{\Psi}{Q}, \frac{(\Psi-1)}{Q} + 1 \right\rceil, \quad k \in \mathbb{Z} \quad (7)$$

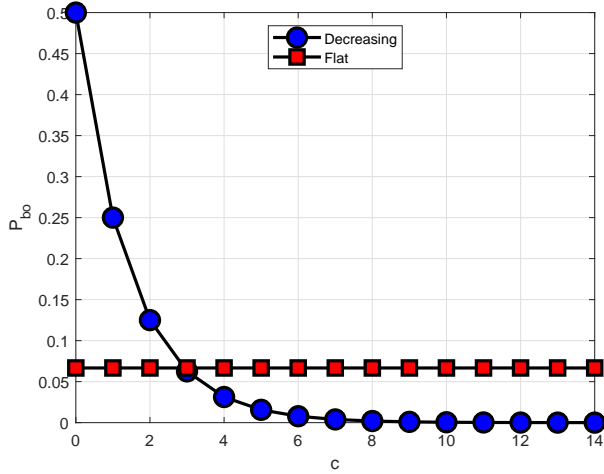


Fig. 2: P_{ini} versus $c \in \{0, 1, \dots, CW - 1\}$ (with $CW = 15$) according to the “decreasing” (proposed) and “flat” (traditional) patterns of backoff counter allocation

Assumption 5 (Fixed k during a backoff allocation process). During a backoff process for a BSM that is shown in Fig. 3, the value of k is assumed to be fixed; in other words, a vehicle does not experience a change of Ψ greater than Q . We assume 10 Hz of the BSM generation frequency—i.e., 10 BSMs per second, which leads to 100 msec per BSM. Notice that a 100 msec is a short time in relation to the reality on the road—i.e., for a vehicle to experience a change in Ψ . Moreover, even if so, as an IEEE 802.11-based system, DSRC is supposed to support such a situation at “best effort.”

We define two types of backoff allocation function versus $c \in \{0, 1, \dots, CW - 1\}$:

Definition 3 (Backoff allocation according to Ψ). *The proposed protocol allocates $P_{bo}(c) := \mathbb{P}[\text{backoff} = c]$ based on the categorization of Ψ into k , as described in Proposition 1 and Fig. 1. The formulation is given by*

$$P_{ini}(c, k) := \mathbb{P}[\text{backoff} = c], \quad \text{where } c \in \{0, 1, \dots, CW - 1\}$$

$$= \begin{cases} r^{c+1} \text{ (“Decreasing”)}, & k > \lceil \frac{K}{2} \rceil \\ \frac{1}{CW} \text{ (“Flat”)}, & k \leq \lfloor \frac{K}{2} \rfloor \end{cases} \quad (8)$$

where term r indicates the intensity of decrease in a $P_{bo}(c)$ and is defined as $r = 1/2$ to make $\sum_{c=0}^{CW-1} P_{ini} = 1$, which is a mathematical requirement to make a Markov chain valid.

More specifically, with a value of k being larger than $\lceil \frac{K}{2} \rceil$ (i.e., the area of “large” Ψ ’s, which indicates cases of greater deviations in a vehicle’s speed), we allocate backoff counters in a “decreasing” pattern. In contrast, for k being smaller than $\lceil \frac{K}{2} \rceil$ (i.e., the area of “small” Ψ ’s, which means cases of smaller deviations in a vehicle’s speed), the backoff counters are allocated in a traditional “flat” fashion in which the probability of any backoff counter value is equal.

Fig. 1 demonstrates an example with $K = 11$ and $Q = 5$. On the PDF, it indicates the principle of the proposed protocol (which shall be described in Section IV): a larger value of $k \in$

$\{1, 2, \dots, K\}$ (which occurs with a smaller probability, $f_S(s)$) takes a smaller backoff value with a higher probability, P_{ini} , as shall be given in (8).

Remark 2 (Interpretation of (8)). *In a “decreasing” backoff allocation, a node is given a higher probability for a smaller backoff value, which increases the chance of winning the medium. A “flat” pattern indicates backoff allocation in a uniform distribution, which is currently adopted by DSRC [21].*

Analyzing Definition 3 further, we can proceed to quantify the probability that a vehicle is allocated a backoff counter following either a decreasing or a flat type function.

Proposition 2 (Probabilities of “decreasing” and “flat” backoff allocation functions). *The proportion of nodes being allocated decreasing and flat patterns of P_{ini} is a predominating factor determining the performance of the proposed system. The proposed protocol determines the proportion by setting a division point in terms of k , to the left and the right of which are assigned for decreasing and flat patterns, respectively. This division can be formally written as*

$$P_{dec} = \int_0^{Q \lceil \frac{K}{2} \rceil} f_{\Psi}(\Psi) d\Psi$$

$$= \int_0^{Q \lceil \frac{K}{2} \rceil} \frac{1}{\sqrt{2\pi}\sigma} \psi^{-\frac{1}{2}} e^{-\frac{\psi}{2\sigma^2}} d\Psi$$

$$= \left[\text{erf} \left(\frac{\sqrt{\Psi}}{\sqrt{2}\sigma} \right) \right]_0^{Q \lceil \frac{K}{2} \rceil}$$

$$= \text{erf} \left(\frac{\sqrt{Q \lceil \frac{K}{2} \rceil}}{\sqrt{2}\sigma} \right) \quad (9)$$

and

$$P_{flat} = \int_{Q \lfloor \frac{K}{2} \rfloor}^{\infty} f_{\Psi}(\Psi) d\Psi$$

$$= \left[\text{erf} \left(\frac{\sqrt{\Psi}}{\sqrt{2}\sigma} \right) \right]_{Q \lfloor \frac{K}{2} \rfloor}^{\infty}$$

$$= 1 - \text{erf} \left(\frac{\sqrt{Q \lfloor \frac{K}{2} \rfloor}}{\sqrt{2}\sigma} \right) \quad (10)$$

where σ denotes the standard deviation of random variable Ψ .

Observing Fig. 1 again, the lefthand and righthand sides of the area under the PDF of Ψ are P_{dec} and P_{flat} , respectively.

It will be worth noticing a few remarks on the proposed protocol, which are given as follows:

Remark 3 (Tx filtering as thinning of Φ). *Such a filtering of Tx vehicles by using the proposed protocol is formulated as a thinning of the PPP Φ . The thinned process has a new intensity, $\tilde{\lambda} \leq \lambda$. The rationale has already been mentioned in Proposition 1. The proposed protocol is expected to grant a higher chance of transmission for vehicles with higher crash risks. As such, when a vehicle’s speed varies too much from*

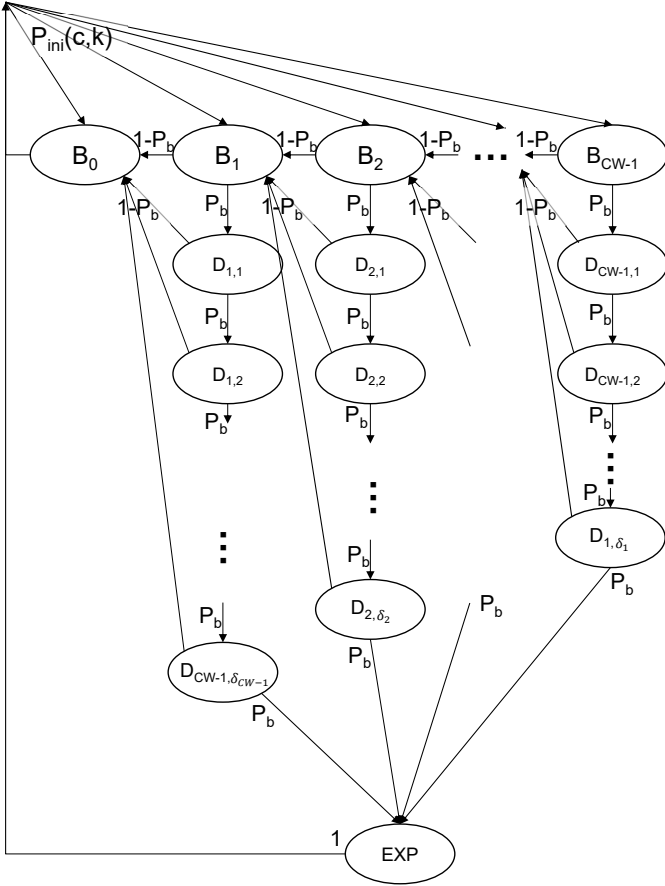


Fig. 3: The proposed protocol as a Markov chain

the speed limit, the vehicle is easily able to broadcast a packet since such a large value of Ψ takes a low probability as shown in Fig. 1.

Remark 4 (Backward compatibility of the proposed protocol). The key benefit of the proposed protocol is modification of the CSMA that is already adopted in DSRC. As such, it will achieve a higher backward compatibility and therefore an easier adoption in practice.

V. STOCHASTIC ANALYSIS

For stochastic analysis, the proposed protocol operated at a vehicle is modeled as a one-dimensional Markov chain as illustrated in Fig. 3. We use fixed-point iterations to solve the model.

A. Markov Chain Representation of DSRC CSMA/CA

To recall, in IEEE 802.11 DCF CSMA/CA [26], if no medium activity is indicated for the duration of a particular backoff slot, then the backoff procedure shall decrement its backoff time by a slot time. If the medium is determined to be busy at any time during a backoff slot, then the backoff procedure is suspended; that is, the backoff timer shall not decrement for that slot. The medium shall be determined to be

idle for the duration of a DIFS period or EIFS, as appropriate, before the backoff procedure is allowed to resume.

As another reminder, the key difference between the traditional DSRC and our proposed backoff allocation scheme lies in P_{ini} . The traditional DSRC adopts the CSMA/CA in which the probability of being allocated a backoff counter is uniform among all the B_c 's with $c \in \{0, 1, \dots, CW - 1\}$. In comparison, the proposed scheme differentiates this probability according to the variation of the speed, Ψ . This makes significant difference in the probability of a packet transmission since, depending on the value of P_b , it can be very difficult to make it through the Markov chain and reach B_0 . Specifically, the proposed protocol allocates higher probabilities of starting the chain from B_c 's with smaller c 's to a vehicle with a larger Ψ . Especially when P_b is higher and thus challenging to propagate toward B_0 , the proposed protocol will significantly prioritize the vehicles with large Ψ 's in the medium competition. Furthermore, as have mentioned in Section I, this is the first work to completely precisely display the effect of an EXP.

In the Markov chain shown in Fig. 3, $D_{c,m}$ where $c \in \{0, 1, \dots, CW - 1\}$ and $m \in \{1, 2, \dots, \delta_c\}$ denotes state of the m th delay at backoff state B_c . The deepest state of a delay, D_{c,δ_c} , means the last possible delay for decrement of the backoff counter from c to $c-1$ before expiration of the packet.

B. Probability of Transmission in a Beacon Period

Let τ denote the probability that a node transmits in any slot within a beaconing period (which is composed of L_{bcn} slots). In other words, τ gives the probability that a node has been able to reach B_0 in the Markov chain after going through the backoff process within a beaconing period without experiencing a packet expiration.

Proposition 3 (Transition matrix of the Markov chain). The transition matrix for the Markov chain (presented in Fig. 3) is denoted by \mathcal{M} , which is formulated in (11) where $\delta_c \in \mathbb{Z}$ gives the maximum number of busy slots that a node can experience before a packet expiration (EXP) at backoff state c , which is formally written as

$$\delta_c = L_{bcn} - l_{bcn} - c \quad (13)$$

with $c \in \{0, 1, \dots, CW - 1\}$. Note that $-l_{bcn}$ comes from the length of a BSM itself, while $-c$ is given from the number of backoffs that has to be decremented. It is noteworthy from (13) that δ_c gets larger with a smaller c , which is translated to that a STA assigned a smaller backoff counter c has a higher chance to reach B_0 .

Proposition 4 (One-step steady-state transition). Let $P_{B_c} = \lim_{t \rightarrow \infty} \mathbb{P}[B(t) = B_c]$, with $B(t)$ giving a backoff counter state at time t and $c \in \{0, 1, \dots, CW - 1\}$, be the stationary distribution of the chain to obtain the steady-state expressions for the Markov chain. A one-step transition between two arbitrary states (i.e., $B_c \rightarrow B_{c-1}$) in steady state for the Markov chain can be formulated as in (12). Note from (a) that the probability of state B_c is composed of two parts: (i) directly from B_0 and (ii) via B_{c+1} . As shown in (b), the

$$\mathcal{M} = \begin{matrix} & B_0 & B_1 & \cdots & B_{CW-1} & D_{1,1} & \cdots & D_{1,\delta_1} & \cdots & D_{CW-1,1} & \cdots & D_{CW-1,\delta_{CW-1}} & EXP \\ \begin{matrix} B_0 \\ B_1 \\ \vdots \\ B_{CW-1} \\ D_{1,1} \\ \vdots \\ D_{1,\delta_1} \\ \vdots \\ D_{CW-1,\delta_1} \\ EXP \end{matrix} & \left[\begin{array}{cccccccccccc} P_{ini}(0,k) & P_{ini}(1,k) & \cdots & P_{ini}(CW-1,k) & 0 & 0 & 0 & \cdots & 0 & 0 & \cdots & 0 & 0 \\ 1-P_b & 0 & \cdots & 0 & P_b & \cdots & 0 & \cdots & 0 & \cdots & 0 & \cdots & 0 \\ \vdots & \vdots & \ddots & \vdots & \vdots & \ddots & \vdots & \ddots & \vdots & \ddots & \vdots & \ddots & \vdots \\ 0 & 0 & \cdots & 0 & 0 & \cdots & 0 & \cdots & P_b & \cdots & 0 & \cdots & 0 \\ 1-P_b & 0 & \cdots & 0 & 0 & \cdots & 0 & \cdots & 0 & \cdots & 0 & \cdots & 0 \\ \vdots & \vdots & \cdots & \vdots & \vdots & \ddots & \vdots & \ddots & \vdots & \cdots & \ddots & \vdots & \vdots \\ 1-P_b & 0 & \cdots & 0 & 0 & \cdots & 0 & \cdots & 0 & \cdots & 0 & \cdots & P_b \\ \vdots & \vdots & \cdots & \vdots & \vdots & \ddots & \vdots & \ddots & \vdots & \ddots & \vdots & \ddots & \vdots \\ 0 & 0 & \cdots & 0 & 0 & \cdots & 0 & \cdots & 0 & \cdots & 0 & \cdots & P_b \\ 0 & 0 & \cdots & 0 & 0 & \cdots & 0 & \cdots & 0 & \cdots & 0 & \cdots & 1 \end{array} \right] \end{matrix} \quad (11)$$

$$\begin{aligned}
& P_{B_{c-1}} \\
& = P_{B_c} \mathbb{P}[B_c \rightarrow B_{c-1}] \\
& \stackrel{(a)}{=} \underbrace{\left[P_{ini}(c,k) + P_{B_{c+1}} \mathbb{P}[B_{c+1} \rightarrow B_c] \right]}_{\substack{=P_{B_c} \\ \text{Directly from } B_0 \quad \text{Via } B_{c+1}}} \mathbb{P}[B_c \rightarrow B_{c-1}] \\
& \stackrel{(b)}{=} \left[P_{ini}(c,k) + \underbrace{\left\{ P_{ini}(c+1,k) + P_{B_{c+2}} \mathbb{P}[B_{c+2} \rightarrow B_{c+1}] \right\}}_{\substack{=P_{B_{c+1}} \\ \text{Directly from } B_0 \quad \text{Via } B_{c+2}}} \right] \mathbb{P}[B_{c+1} \rightarrow B_c] \mathbb{P}[B_c \rightarrow B_{c-1}] \\
& = \left[P_{ini}(c,k) + \left\{ P_{ini}(c+1,k) + \underbrace{\left(P_{ini}(c+2,k) + P_{B_{c+2}} \mathbb{P}[B_{c+3} \rightarrow B_{c+2}] \right)}_{\substack{=P_{B_{c+2}} \\ \text{Directly from } B_0 \quad \text{Via } B_{c+2}}} \right\} \mathbb{P}[B_{c+2} \rightarrow B_{c+1}] \right] \mathbb{P}[B_{c+1} \rightarrow B_c] \mathbb{P}[B_c \rightarrow B_{c-1}] \\
& \stackrel{(c)}{=} \left[P_{ini}(c,k) + \left\{ P_{ini}(c+1,k) + \underbrace{\left(P_{ini}(c+2,k) + P_{B_{c+2}} (1-P_b) \right)}_{\substack{=P_{B_{c+2}} \\ \text{Directly from } B_0 \quad \text{Via } B_{c+2}}} \right\} (1-P_b) \right] (1-P_b) \\
& \stackrel{(d)}{=} \text{The expansion is kept until reaching } \mathbb{P}[B_{CW-1}] \quad (12)
\end{aligned}$$

same holds for B_{c+1} , from which one can infer the pattern of steady-state propagation for the Markov chain. Also, in (c), we substitute $\mathbb{P}[B_c \rightarrow B_{c-1}]$ with $1 - P_b$ as illustrated in Fig. 3. Lastly, (d) tells that the expansion shown in (12) goes until it reaches $\mathbb{P}[B_{CW-1}]$. It is important to note that state B_{CW-1} has only one input: directly from B_0 .

Now, the following two propositions present the formulation of a numerical solution for τ and P_b .

Proposition 5 (τ as a function of P_b). *The probability of reaching state B_0 is equivalent to the probability of a packet transmission after propagating through the Markov chain [23]. The general one-step steady-state transition shown in Proposition 4 can be applied to obtain the probability of transition from an arbitrary state B_c to P_{B_0} . In this paper, this transition formula provides a piece for the numerical solve of*

τ and P_b , which is given by

$$\begin{aligned}
\tau & := P_{B_0} \\
& = P_{B_1} \underbrace{(1 - P_b)}_{= \mathbb{P}[B_1 \rightarrow B_0]} \\
& = \left(P_{ini}(1,k) + P_{B_2} \underbrace{(1 - P_b)}_{= \mathbb{P}[B_2 \rightarrow B_1]} \right) (1 - P_b) \\
& = \left(P_{ini}(1,k) + (P_{ini}(2,k) + \cdots) (1 - P_b) \right) (1 - P_b). \quad (14)
\end{aligned}$$

Implication of (14) is that now tau is written as a function of P_b since all the $P_{ini}(c,k)$'s are known.

Proposition 6 (τ as a function of P_b and n_{cs}). *While the Markov chain describes a node's process of going through a backoff process in CSMA/CA, P_b is determined from the dynamics among the nodes competing for the channel. More specifically, all the nodes that are located in the carrier-sense*

range of the tagged vehicle become the competitors for the channel. The probability of a slot being found busy can be formulated as

$$P_b = 1 - (1 - \tau)^{n_{cs}} \quad (15)$$

where n_{cs} denotes the number of nodes within a given node's range of carrier sensing.

Lemma 2 (Numerical solution for τ). *We compute τ and P_b via numerical solve based on simultaneous equations composed of (14) and (15) that have been presented in Propositions 5 and 6, respectively. The simultaneous equations were to be solved via a sufficiently large number of iterations testing all the possible values for τ and P_b .*

C. Packet Delivery Rate (PDR)

Appreciating its easiness to understand, this paper adopts the probability that a packet is successfully delivered to an arbitrary receiver vehicle (or PDR) as the key metric evaluating the proposed protocol in comparison to the original DSRC.

Lemma 3 (Probability of an EXP). *The probability that a node is not able to transmit in any slot within a beaconing period can be formulated as*

$$P_{exp} = 1 - \tau \quad (16)$$

Proof: It is significant to note that a backoff process of DSRC is “reset” after every beaconing period regardless of whether a packet is successfully transmitted or not. It means that the “steady-state” in DSRC is $t \approx L_{bcn} \times (\text{Slot time})$ rather than $t \rightarrow \infty$ as in other IEEE 802.11 standards. As such, cases of finishing at other states including B 's and D 's occur although a separate state of EXP exists in the backoff process model as shown in Fig. 3. Recall from Fig. 3 that state D_{c,δ_c} , the deepest state of a delay with backoff counter c , gives the last possible delay state before being drained to an EXP. It implies the possibility of staying at any other state than B_0 and EXP at the end of a beaconing period, which consequently should be added to the probability of an EXP. As a consequence, the probability of an EXP is obtained as $P_{exp} = 1 - \tau$. ■

Once a packet is transmitted, in order to lead to a successful delivery, no collision must occur on the packet during the transit. In other words, for a tagged vehicle, an external collision occurs unless both of the following conditions are satisfied: (1) when the tagged vehicle is transmitting, no vehicles within its carrier-sensing range delivery packets at the same time slot; and (2) when the tagged vehicle is transmitting, no hidden terminals should corrupt the tagged vehicle's packet.

To formulate, as just have mentioned, there are two types of collision in an IEEE 802.11-based network—namely, SYNC and HN [42]. Notice that the geometry for a SYNC is limited to the tagged vehicle's carrier-sense range because the packet collision occurs among the vehicles who are sensed but cannot avoid a collision due to allocation of a same backoff value [21]. On the other hand, the geometry for a HN is greater than a SYNC because the vehicles causing this type of packet

collision are placed outside of the tagged vehicle's carrier-sense range [21], which figuratively defines “hidden nodes.”

Lemma 4 (Probability of a SYNC). *The probability that a packet collides over the air due to a synchronized collision is given by*

$$P_{sync}(n_{cs}, CW) = 1 - \sum_{n_{tx}=0}^{n_{cs}} \left[[n_{tx} \leq CW] \binom{n_{cs}}{n_{tx}} \tau^{n_{tx}} (1 - \tau)^{n_{cs} - n_{tx}} \frac{CW!}{(CW - n_{tx})! CW^{n_{tx}}} \right] \quad (17)$$

Proof: Let us define the probability of a SYNC as

$$P_{sync}(n_{cs}, CW) = 1 - \mathbb{P}[\text{No SYNC} \mid n_{cs} > 0]. \quad (18)$$

Assuming independence between two events forming the condition relationship in (18), we can rewrite as

$$\begin{aligned} & \mathbb{P}[\text{No SYNC} \mid n_{cs} > 0] \\ &= \mathbb{P}[\text{No SYNC}] \mathbb{P}[n_{cs} > 0] \\ &\stackrel{(a)}{\approx} \mathbb{P}[\text{No SYNC}] \\ &= \sum_{n_{tx}=0}^{n_{cs}} \left([n_{tx} \leq CW] \mathbb{P}[n_{tx} \text{ Tx's}] \right. \\ &\quad \left. \mathbb{P}[\text{All different backoffs among them}] \right) \quad (19) \end{aligned}$$

where $[n_{tx} < CW]$ gives an Iverson bracket:

$$[n_{tx} \leq CW] = \begin{cases} 1, & n_{tx} \leq CW \\ 0, & \text{otherwise} \end{cases} \quad (20)$$

It indicates that in order for a SYNC not to occur, there must be only $n_{tx} \leq CW$ STAs transmitting, which leaves a possibility that all STAs are assigned all different backoff values. In other words, a SYNC can never be avoided when $n_{tx} > CW$ STAs compete for the medium.

Step (a) comes from the following rationale. A key condition for a point process to be a PPP is that the number of points falling in a bounded Borel set \mathcal{A} is a Poisson random variable with the parameter of $\lambda|\mathcal{A}|$ [61] where $|\mathcal{A}|$ denotes the area of an arbitrary two-dimensional space \mathcal{A} . Refer to Figs. 6 and 7 of [21] that A_{col} forms a circular space in which a point x is located at the origin of the center and another point y is placed r away from the origin. That is, $|A_{col}| = \pi r_{cs}^2$. Based on this, we can exploit the CDF of the distance l between the two arbitrary points for calculation of $1 - \mathbb{P}(\text{No other node in } A_{col})$, which is written as

$$\begin{aligned} & \mathbb{P}(n_{cs} > 0) \stackrel{(b)}{=} \mathbb{P}(n > 0, A_{col}) \\ &= 1 - \mathbb{P}(n_{cs} = 0, A_{col}) \\ &= 1 - \frac{(\lambda \pi r_{cs}^2)^0 e^{-\lambda \pi r_{cs}^2}}{0!} \\ &= 1 - e^{-\lambda \pi r_{cs}^2}, \quad r_{cs} \geq 0. \quad (21) \end{aligned}$$

For (b), we assume the existence of two nodes at least: one for vT and the other as a potential SYNC-causing node. Here,

it is important to note that with a realistic value for r_{cs} , $\mathbb{P}(n_{cs} > 0) \approx 1$. This justifies approximation (a) in (19).

Now, we present specifics for each term of (19). It is worth to note from the summation in (19) that we consider every possible number of actually transmitting STAs (i.e., n_{tx}) among all the STAs sensed by the tagged vehicle's (i.e., n_{cs}).

The first term inside the summation of (19) is elaborated as

$$\mathbb{P}[n_{tx} \text{ Tx's}] = \binom{n_{cs}}{n_{tx}} \tau^{n_{tx}} (1 - \tau)^{n_{cs} - n_{tx}} \quad (22)$$

with τ as has been given in Proposition 5.

The second term inside the summation in (19) indicates the probability that all the n_{tx} vehicles ($\forall 0, 1, \dots, n_{cs}$) are assigned different backoff counter values, which is given by

$$\begin{aligned} & \mathbb{P}[\text{All different backoffs among them}] \\ &= \frac{\text{All different backoff selections}}{\text{All possible backoff selections by } n_{Tx} \text{ STAs}} \\ &= \frac{\text{CW!} [(CW - n_{tx})!]^{-1}}{\text{CW}^{n_{tx}}} \quad (23) \end{aligned}$$

This yields

$$\begin{aligned} & \mathbb{P}[\text{No SYNC} \mid n_{cs} > 0] \\ &= \sum_{n_{tx}=0}^{n_{cs}} \left[[n_{tx} \leq \text{CW}] \binom{n_{cs}}{n_{tx}} \tau^{n_{tx}} (1 - \tau)^{n_{cs} - n_{tx}} \right. \\ & \quad \left. \frac{\text{CW!}}{(\text{CW} - n_{tx})! \text{CW}^{n_{tx}}} \right] \quad (24) \end{aligned}$$

Therefore, the probability of a SYNC can be formulated as

$$\begin{aligned} & P_{\text{sync}}(n_{cs}, \text{CW}) \\ &= 1 - \sum_{n_{tx}=0}^{n_{cs}} \left[[n_{tx} \leq \text{CW}] \binom{n_{cs}}{n_{tx}} \tau^{n_{tx}} (1 - \tau)^{n_{cs} - n_{tx}} \right. \\ & \quad \left. \frac{\text{CW!}}{(\text{CW} - n_{tx})! \text{CW}^{n_{tx}}} \right] \quad (25) \end{aligned}$$

which completes the proof. \blacksquare

Lemma 5 (Probability of a HN). *The probability that a packet collides over the air due to a synchronized collision is given by*

$$\begin{aligned} & P_{\text{hn}}(n_{hn}, \text{CW}) \\ &= 1 - \sum_{n_{tx}=0}^{n_{cs}} \left[[n_{tx} \leq \text{CW}] \binom{n_{cs}}{n_{tx}} \tau^{n_{tx}} (1 - \tau)^{n_{cs} - n_{tx}} \right. \\ & \quad \left. \mathbb{E}_c \left[\left(\frac{|\mathcal{S}_{\sim \text{hn}}|}{\text{CW}} \right)^{n_{tx}} \right] \right] \quad (26) \end{aligned}$$

Proof: Before starting derivation of an equation, it is significant to discuss the critical difference between a SYNC and a HN. While a SYNC occurs in a single slot, a HN can occur at any time instant within an entire BSM (i.e., l_{bcn} slots), since the colliding STAs are unable to sense each other in a HN situation. Specifically, there are two possible scenarios in which a hidden terminal causes a collision with

the tagged vehicle: (i) the tagged vehicle starts sending while a hidden terminal is transmitting, or (ii) a hidden terminal starts sending while the tagged vehicle is transmitting. As such, the key difference is that unlike a SYNC, a HN collision can occur even when the STAs transmitting colliding packets were assigned different backoff values.

We start the formulation in a similar way to P_{sync} that was shown in (18), which is given by

$$P_{\text{hn}}(n_{hn}, \text{CW}) = 1 - \mathbb{P}[\text{No HN} \mid n_{cs} > 0] \quad (27)$$

where

$$\begin{aligned} & \mathbb{P}[\text{No HN} \mid n_{cs} > 0] \\ & \stackrel{(a)}{\approx} \mathbb{P}[\text{No HN}] \\ &= \sum_{n_{tx}=0}^{n_{cs}} \left([n_{tx} \leq \text{CW}] \mathbb{P}[n_{tx} \text{ Tx's}] \right. \\ & \quad \left. \mathbb{P}[\text{No hidden terminal transmission}] \right) \quad (28) \end{aligned}$$

Approximation (a) is based on the same rationale as one given in (19).

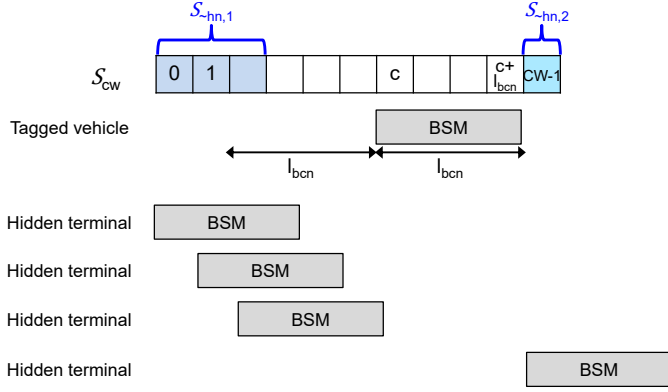
Also, the same Iverson bracket with one shown (19), i.e., $[n_{tx} \leq \text{CW}]$, is given as the first term inside the summation. That is, if the number of transmitting hidden terminals exceeds the current CW, there is no chance that the tagged vehicle can avoid a HN since the existence of hidden terminals.

The second term has also been derived in (22). The only difference here is that n_{cs} is replaced with $n_{hn} = 3n_{cs}$ assuming the same density. The reason is that the area of a HN has been found as a donut-shaped region formed between circumferences with the radii of r_{cs} and $2r_{cs}$ as illustrated in Fig. 17 of [21].

The last term in (28) is found as follows. Let \mathcal{S}_{cw} denote the set of bakcoff values for a given CW, i.e., $\mathcal{S}_{\text{cw}} := \{0, 1, \dots, \text{CW} - 1\}$. Fig. 4 illustrates an example scenario of no HN: a hidden terminal's packet does not overlap with the tagged vehicle's. Sets $\mathcal{S}_{\sim \text{hn},1}$ and $\mathcal{S}_{\sim \text{hn},2}$ contain backoff values (before and after the tagged vehicle's packet, respectively), with which a hidden terminal does not collide with the tagged vehicle, where $\mathcal{S}_{\sim \text{hn},1}, \mathcal{S}_{\sim \text{hn},2} \subset \mathcal{S}_{\text{cw}}$. That way, we define the set of all possible backoff values for a hidden terminal without causing a HN as $\mathcal{S}_{\sim \text{hn}} = \mathcal{S}_{\sim \text{hn},1} \cup \mathcal{S}_{\sim \text{hn},2}$. Based on the definition, we now can derive the term that we are trying to find as

$$\mathbb{P}[\text{No hidden terminal transmission}] = \mathbb{E}_c \left[\left(\frac{|\mathcal{S}_{\sim \text{hn}}|}{\text{CW}} \right)^{n_{tx}} \right] \quad (29)$$

It is critical to note that $\mathcal{S}_{\sim \text{hn}}$ depends on which backoff value c the tagged vehicle is assigned, as shown in Fig. 4. This is the reason that an average $\mathbb{E}[\cdot]_c$ is needed.

Fig. 4: An example of $\mathcal{S}_{\sim hn}$

This leads to

$$\begin{aligned} & \mathbb{P}[\text{No HN} \mid n_{cs} > 0] \\ &= \sum_{n_{tx}=0}^{n_{cs}} \left[[n_{tx} \leq \text{CW}] \binom{n_{cs}}{n_{tx}} \tau^{n_{tx}} (1-\tau)^{n_{cs}-n_{tx}} \right. \\ & \quad \left. \mathbb{E}_c \left[\left(\frac{|\mathcal{S}_{\sim hn}|}{\text{CW}} \right)^{n_{tx}} \right] \right] \quad (30) \end{aligned}$$

Therefore, the probability of a HN can be formulated as

$$\begin{aligned} & P_{hn}(n_{hn}, \text{CW}) \\ &= 1 - \sum_{n_{tx}=0}^{n_{cs}} \left[[n_{tx} \leq \text{CW}] \binom{n_{cs}}{n_{tx}} \tau^{n_{tx}} (1-\tau)^{n_{cs}-n_{tx}} \right. \\ & \quad \left. \mathbb{E}_c \left[\left(\frac{|\mathcal{S}_{\sim hn}|}{\text{CW}} \right)^{n_{tx}} \right] \right] \quad (31) \end{aligned}$$

which completes the proof. \blacksquare

Theorem 1 Based on the parameters defined through this paper, the PDR is formulated as

$$\text{PDR} = \tau (1 - P_{\text{col}}) \quad (32)$$

where

$$P_{\text{col}} = P_{\text{sync}} (1 - P_{\text{hn}}) + P_{\text{hn}} (1 - P_{\text{sync}}) + P_{\text{sync}} P_{\text{hn}} \quad (33)$$

Proof:

$$\begin{aligned} \text{PDR} &= \mathbb{P}[\text{No collision over the air} \mid \text{Packet transmission}] \\ &\stackrel{(a)}{=} P_{\text{col}} \tau \quad (34) \end{aligned}$$

where (a) follows from the assumption that the two events, “No collision over the air” and “Packet transmission,” are independent.

Also, notice that P_{col} gives the probability of collision which is formulated as

$$\begin{aligned} P_{\text{col}} &= \mathbb{P}[\text{SYNC only}] + \mathbb{P}[\text{HN only}] + \mathbb{P}[\text{Both SYNC and HN}] \\ &= P_{\text{sync}} (1 - P_{\text{hn}}) + P_{\text{hn}} (1 - P_{\text{sync}}) + P_{\text{sync}} P_{\text{hn}} \quad (35) \end{aligned}$$

Substituting (35) into (34) completes the proof. \blacksquare



Fig. 5: Formulation of IRT as a geometric distribution

D. IRT

The second metric through which the performance of the proposed protocol is evaluated is the IRT. Fig. 5 illustrates the formulation of an IRT as a geometric distribution.

Notice that the unit of a quantity of IRT is “the number of slots.” As such, one needs to multiply a slot time when needing to display an IRT in the unit of time (i.e., seconds).

Lemma 6 (Distribution of IRT). *As aforementioned, the probability that an IRT occurs in the next k th beaconing period after the last successful delivery follows a geometric distribution, which can be formally written as*

$$\text{IRT} = (1 - \text{PDR})^{\nu-1} \text{PDR} \quad (36)$$

where ν denotes the number of unsuccessful receptions.

Proof: For occurrence of an “IRT,” we suppose to start from a successful reception, then measure how many beaconing periods are needed until the next successful reception. This is the reason that in Fig. 5, the first beaconing period is set to have the probability of PDR, and thereafter the possibility is left open between PDR and $1 - \text{PDR}$. It is formally written as

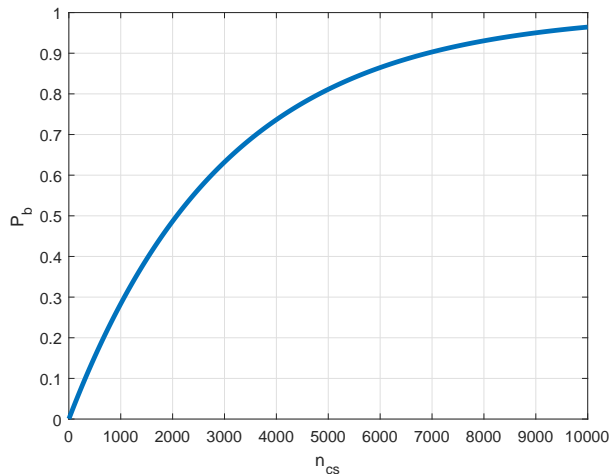
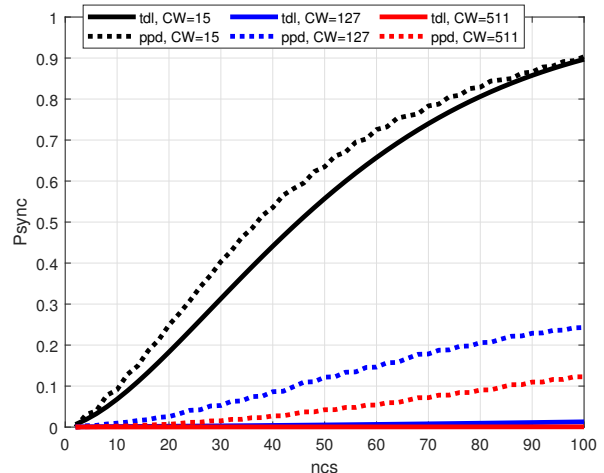
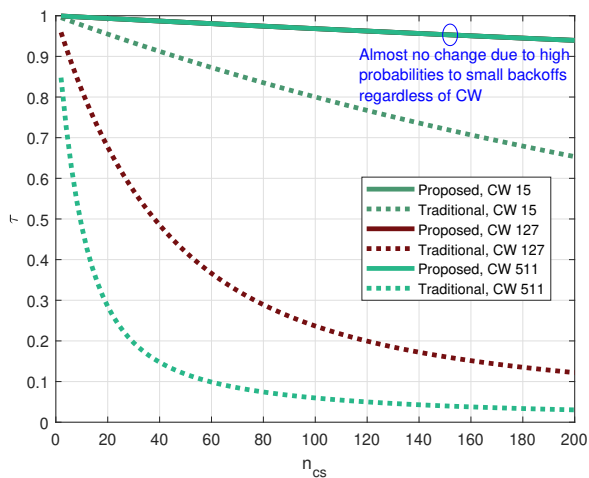
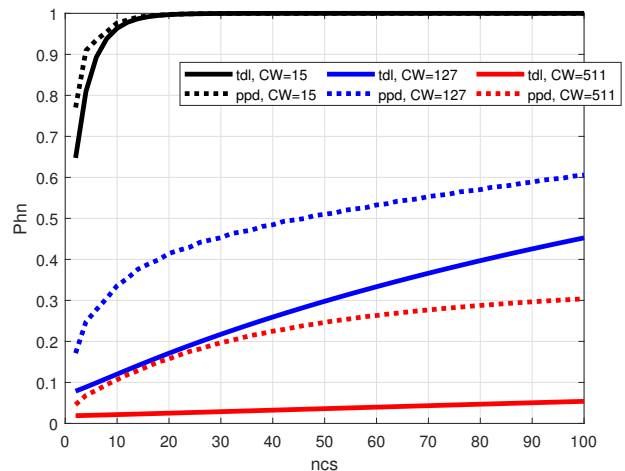
$$\begin{aligned} \text{IRT} &\sim \text{Geo}(\text{PDR}) \\ &= \mathbb{P}[\text{IRT} = \nu] \\ &= (1 - \text{PDR})^{\nu-1} \text{PDR} \quad (37) \end{aligned}$$

VI. RESULTS AND DISCUSSIONS

This section verifies the accuracy of the analysis presented in Section V, by comparing to Monte Carlo simulations of the network defined in Section III.

A. Results

1) P_b : Fig. 6 demonstrates the P_b that has been resulted from the “uniform” approximated τ . Overall, the probability that a certain slot is found busy with another node can be kept relatively low—i.e., around 15% even with 500 competing nodes within one’s carrier-sense range. The reason is the small value for τ as shown in Fig. 7, which is plausible because a beaconing period contains a very large number of slots—i.e., L_{bcn} is as large as 750 with 50 msec and 66.7 μsec for a beaconing period and a slot time, respectively. The numbers $L_{bcn} = 750$ and time length of 50 msec come from the fact that a CCH takes 50 msec of an entire 100-msec beaconing

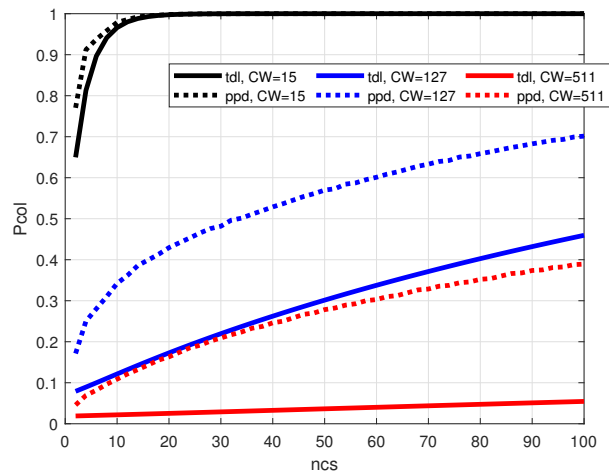
Fig. 6: P_b versus n_{cs} Fig. 8: P_{sync} versus n_{cs} Fig. 7: τ versus n_{cs} Fig. 9: P_{hn} versus n_{cs}

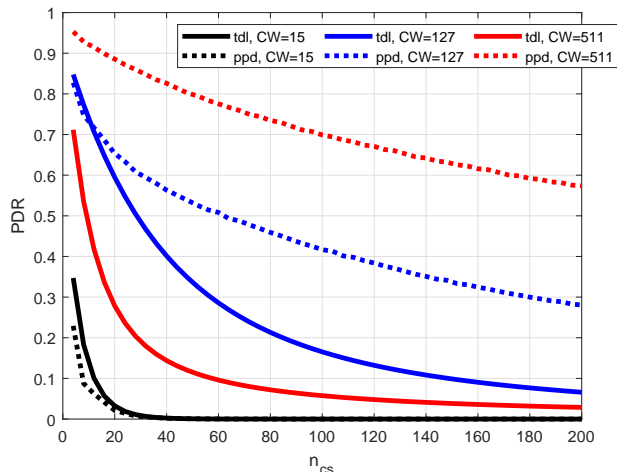
period, based on IEEE 1609.4 that defines the “alternation” between CCH and SCH [62].

Also, the results match one’s intuitions: P_b is increased with a greater n_{cs} . One can observe that a smaller value of r yields a lower P_b (which, in turn, leads to a higher P_{start} as such). The rationale behind this result is that a smaller r serves as a more drastic decrement of P_{ini} as shown in (8).

2) τ : Fig. 7 shows the probability that a vehicle has been able to go through a backoff process and transmit a BSM, denoted by τ , versus the number of vehicles within its carrier-sense range. Notice that the key change from the reference [21] is the Markov chain due to proposition of P_{ini} .

3) P_{col} : Figs. 8 and 9 demonstrate the probabilities of collision by a SYNC and HN, respectively, while Fig. 10 presents the resulting probability of a collision, which was given in (35). The probabilities are displayed versus n_{cs} according to the backoff function type and CW. There are several important points to discuss from Figs. 8 and 9: (i) a larger CW is effective in alleviating both SYNC and HN, and therefore P_{col} as a direct consequence; (ii) For a CW,

Fig. 10: P_{col} versus n_{cs}

Fig. 11: PDR versus n_{cs}

$P_{hn} > P_{sync}$ with a node density. The reasoning is that the number of hidden terminals is larger than that of STAs causing a SYNC since the area of HN is larger than that of SYNC [21]; (iii) the proposed protocol yields a higher P_{col} than the traditional CSMA/CA since, on average, it allows certain nodes more likely to transmit.

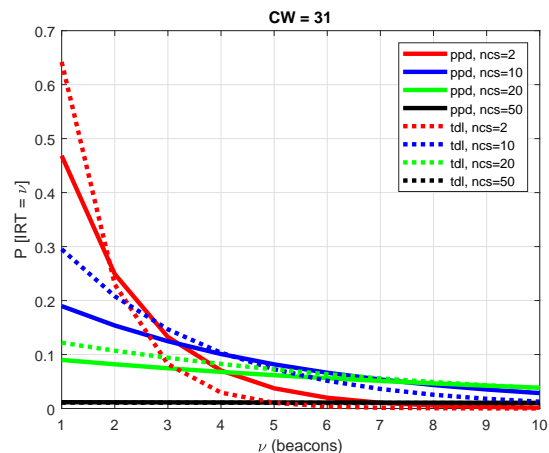
4) PDR: Fig. 11 shows PDR versus n_{cs} . We note two key observations as follows. First, the proposed protocol yields a higher PDR while it showed an unfavorable P_{col} , the reason of which is interpreted as a higher margin in τ . Second, the margin that the proposed protocol yields in PDR gets increased with a larger CW. The reason is that P_{col} gets very small (i.e., ≈ 0) with a larger CW such as 511.

5) IRT: Fig. 12 shows the probability mass function (PMF) of IRT with respect to ν , the number of slots until the next successful packet delivery. Comparing 12a and 12b suggests that a larger CW results in a higher probability of smaller IRTs, which is attributed to a higher PDR with a larger CW as shown in Fig. 11. Within each of 12a and 12b, it is observed that a smaller n_{cs} yields a higher probability of smaller IRTs. The proposed protocol underperforms the traditional CSMA with CW = 31 as seen in Fig. 12a because of the same tendency in PDR. In contrast, with a large CW (i.e., CW = 511), the outperformance of the proposed protocol gets significant with all given values of n_{cs} .

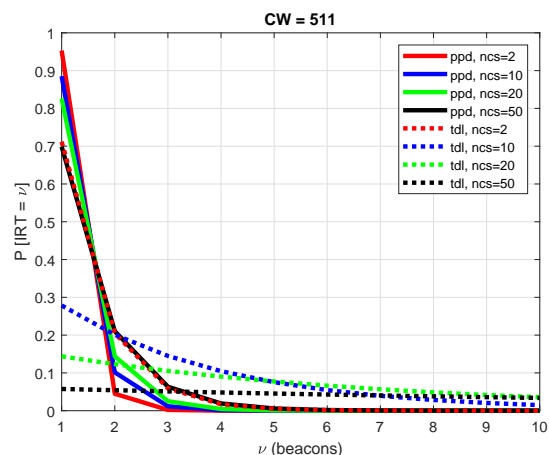
B. Discussions

The proposed scheme yields a higher performance compared to the proposed mechanism in terms of PDR and IRT as shown in Figs. 11 and 12, respectively. The reason of a higher PDR achieved by the proposed scheme, despite a higher P_{col} as found in Fig. 10, is attributed to a higher τ as Fig. 7 presents.

The predominance of CW in determination of PDR and IRT suggests that P_{col} acts as the most critical factor in inducing the two quantities. As observed in Fig. 10, a larger CW yields a lower P_{col} and broadens the outperformance of the proposed scheme over the proposed one. Henceforth, all these results



(a) CW = 31



(b) CW = 511

Fig. 12: IRT versus ν

suggest that a DSRC network can actively increase CW as an effort to combat a lower PDR as a result of high road traffic, i.e., a large n_{cs} .

VII. CONCLUSIONS

This paper proposed a backoff allocation scheme that is adaptive to the level of accident risk to which a vehicle is exposed. The proposed scheme requires a minimal modification of the current CSMA mechanism adopted for IEEE 802.11p, which can achieve higher generality and applicability to practice. We first identified the driving speed as a key factor determining a crash risk. For analysis, we defined the variance of speed as the key metric and presented closed-form expressions for the probability distribution of the metric. Then, we modeled the IEEE 802.11p CSMA as a Markov process, from which further performance evaluation metrics were derived: i.e., probabilities of transmission within a beaconing period, transmission within a certain slot, collision by a SYNC, collision by a HN, and IRT. From the analysis and numerical results, the main finding was that the performance of a BSM broadcast in an IEEE 802.11p network is predominated by contention rather than collision.

As such, this work has many possible extensions. The key merit of this work is identification of a factor that is critical in causing an accident among the ones that can be obtained on a vehicle autonomously without any external support from infrastructure (e.g., RSU), which fits the “distributed” nature of a V2X network. One possible extension is to examine the feasibility of the proposed mechanism for a completely distributed consensus algorithm (e.g., practical Byzantine fault tolerance) for blockchain. Considering that the decentralization is being regarded as one of the most critical factors in the blockchain, the complete decentralization achieved by the proposed scheme will form a critical basis for establishing analytical frameworks for such blockchain-related extension.

REFERENCES

- [1] US FCC, *Dedicated short range communications (DSRC) service*, Apr. 2019. [Online]. Available: <https://www.fcc.gov/wireless/bureau-divisions/mobility-division/dedicated-short-range-communications-dsrc-service>
- [2] US FCC, *The commission seeks to update and refresh the record in the “unlicensed national information infrastructure (U-NII) devices in the 5 GHz band” Proceeding*, FCC 16-68A1.
- [3] 5GAA, “The case for cellular V2X for safety and cooperative driving,” Nov. 2016. [Online]. Available: <http://5gaa.org/wp-content/uploads/2017/10/5GAA-whitepaper-23-Nov-2016.pdf>
- [4] K. Bode, “5G could actually make the ‘digital divide’ worse,” *Techdirt Wireless*, Feb. 2020. [Online]. Available: <https://www.techdirt.com/articles/20200204/07071543850/5g-could-actually-make-digital-divide-worse.shtml>
- [5] J. Van Roy, “EU parliament finally votes for wifi to connect cars,” *New Mobility News*, Apr. 2019. [Online]. Available: <https://newmobility.news/2019/04/18/eu-parliament-finally-votes-for-wifi-to-connect-cars/>.
- [6] AASHTO, “State DOTs sign letter supporting preservation of 5.9 GHz spectrum,” *AASHTO J.*, Aug. 2019. [Online]. Available: <https://aashtojournal.org/2019/08/23/state-dots-sign-letter-supporting-preservation-of-5-9-ghz-spectrum/>.
- [7] US FCC, “Phase I testing of prototype U-NII-4 devices,” *TR 17-1006*, Oct. 2018.
- [8] AASHTO, *Re: Docket No. DOT-OST-2018-0210*, Feb. 2019. [Online]. Available: <https://policy.transportation.org/wp-content/uploads/sites/59/2019/02/AASHTO-Comments-USDOT-V2X-Communication-RFC-FINAL.pdf>
- [9] A. Weinfeld, “Methods to reduce DSRC channel congestion and improve V2V communication reliability,” in *Proc. ITS World Congress 2010*.
- [10] US FCC, “In the matter of use of the 5.850-5.925 GHz band,” *Notice of Proposed Rulemaking*, ET Docket No. 19-138, FCC 19-129, Dec. 2019.
- [11] S. Kim, J. Park, and K. Bian, “PSUN: An OFDM transmission strategy for coexistence with pulsed radar,” in *Proc. IEEE ICNC 2015*.
- [12] S. Kim, J. Choi, and C. Dietrich, “PSUN: an OFDM - pulsed radar coexistence technique with application to 3.5 GHz LTE,” *Hindawi Mobile Inform. Syst. J.*, Jul. 2016.
- [13] S. Kim, J. Choi, and C. Dietrich, “Coexistence between OFDM and pulsed radars in the 3.5 GHz band with imperfect sensing,” in *Proc. IEEE WCNC 2016*.
- [14] S. Kim and C. Dietrich, “Coexistence of outdoor Wi-Fi and radar at 3.5 GHz,” *IEEE Wireless Commun. Lett.*, vol. 6, iss. 4, Aug. 2017.
- [15] S. Kim, E. Visotsky, P. Moorut, K. Bechta, A. Ghosh, and C. Dietrich, “Coexistence of 5G with the incumbents in the 28 and 70 GHz bands,” *IEEE J. Sel. Areas Commun.*, vol. 35, iss. 8, Aug. 2017.
- [16] M. Kabir and S. Kim, “5G or Wi-Fi for HA/DR in the 60 GHz Band?,” in *Proc. IEEE Int. Symp. Technol. Homeland Security 2019*.
- [17] J. Verboom and S. Kim, “Stochastic analysis on downlink performance of coexistence between WiGig and NR-U in 60 GHz band,” *arXiv:2003.01570*, Mar. 2020.
- [18] S. Kim and T. Dessalgn, “Mitigation of civilian-to-military interference in DSRC for urban operations,” in *Proc. IEEE MILCOM 2019*.
- [19] S. Kim and B. J. Kim, “Prioritization of basic safety message in DSRC based on distance to danger,” *arXiv:2003.09724*, Mar. 2020.
- [20] J. W. Tantra, C. H. Foh, and A. Ben Mnaouer, “Throughput and delay analysis of the IEEE 802.11e EDCA saturation,” in *Proc. IEEE ICC 2005*.
- [21] S. Kim and M. Bennis, “Spatiotemporal analysis on broadcast performance of DSRC with external interference in 5.9 GHz band,” *arXiv:1912.02537*, Dec. 2019. [Online]. Available: <https://arxiv.org/pdf/1912.02537.pdf>
- [22] S. Kim, “Impacts of mobility on performance of blockchain in VANET,” *IEEE Access*, vol. 7, May 2019.
- [23] G. Bianchi, “IEEE 802.11–saturation throughput analysis,” *IEEE Commun. Lett.*, vol. 12, no. 2, Dec. 1998.
- [24] X. Yin, X. Ma, and K. S. Trivedi, “An interacting stochastic models approach for the performance evaluation of DSRC vehicular safety communication,” *IEEE Trans. Comput.*, vol. 62, no. 5, May 2013.
- [25] IEEE 802.11p Standard, “802.11p-2010 - IEEE Standard for Information technology– Local and metropolitan area networks– Specific requirements– Part 11: Wireless LAN Medium Access Control (MAC) and Physical Layer (PHY) Specifications Amendment 6: Wireless Access in Vehicular Environments,” Jun. 2010.
- [26] IEEE 802.11 Standard, “802.11-2016 - IEEE Standard for Information technology–Telecommunications and information exchange between systems Local and metropolitan area networks–Specific requirements - Part 11: Wireless LAN Medium Access Control (MAC) and Physical Layer (PHY) Specifications,” Dec. 2016.
- [27] Y. Yao, L. Rao, X. Liu, “Performance and reliability analysis of IEEE 802.11p safety communication in a highway environment,” *IEEE Trans. Veh. Technol.*, vol. 62, no. 9, 2013.
- [28] M. Khabazian, S. Aissa, M. Mehmet-Ali, “Performance modeling of safety messages broadcast in vehicular ad hoc networks,” *IEEE Trans. Intell. Transp. Syst.*, vol. 14, no. 1, 2013.
- [29] X. Lei and S. H. Rhee, “Performance analysis and enhancement of IEEE 802.11p beaconing,” *EURASIP J. Wireless Commun. Netw.*, vol. 2019, no. 61, Dec. 2019.
- [30] S. Son and K.-J. Park, “BEAT: beacon inter-reception time ensured adaptive transmission for vehicle-to-vehicle safety communication,” *MDPI Sensors*, vol. 19, no. 14, Jul. 2019.
- [31] T. ElBatt, S. K. Goel, G. Holland, H. Krishnan, and J. Parikh, “Cooperative collision warning using dedicated short range wireless communications,” in *Proc. ACM VANET 2006*.
- [32] G. Jornod, A. El Assaad, A. Kwoczek, and T. Kurner, “Packet inter-reception time modeling for high-density platooning in varying surrounding traffic density,” in *Proc. IEEE EuCNC 2019*.
- [33] T. T. Almeida, L. de C. Gomes, F. M. Ortiz, J. G. R. Junior, and L. H. M. K. Costa, “IEEE 802.11p performance evaluation: simulations vs. real experiments,” in *Proc. IEEE ISTC 2018*.
- [34] B. Cheng, H. Lu, A. Rostami, M. Gruteser, and J. B. Kenney, “Impact of 5.9 GHz spectrum sharing on DSRC performance,” in *Proc. IEEE VNC 2017*.
- [35] I. Khan, G. M. Hoang, and J. Harri, “Rethinking cooperative awareness for future V2X safety-critical applications,” in *Proc. IEEE VNC 2017*.
- [36] Z. Liu, Z. Liu, Z. Meng, X. Yang, L. Pu, and L. Zhang, “Implementation and performance measurement of a V2X communication system for vehicle and pedestrian safety,” *Internat. J. Distributed Sensor Netw.*, vol. 12, no. 9, Sep. 2016.
- [37] M. E. Rendaa, G. Restaa, P. Santi, F. Martelli, and A. Franchini, “IEEE 802.11p VANets: experimental evaluation of packet inter-reception time,” *Elsevier Comput. Commun.*, vol. 75, Feb. 2016.
- [38] M. Torrent-Moreno, J. Mittag, P. Santi, and H. Hartenstein, “Vehicle-to-vehicle communication: Fair transmit power control for safety-critical information,” *IEEE Trans. Veh. Technol.*, vol. 58, no. 7, Mar. 2009.
- [39] B. Kloiber, J. Harri, T. Strang, S. Sand, and C. R. Garcia, “Random transmit power control for DSRC and its application to cooperative safety,” *IEEE Trans. Dependable Secur. Comput.*, vol. 13, no. 1, Jun. 2015.
- [40] C. L. Huang, Y. P. Fallah, R. Sengupta, and H. Krishnan, “Intervehicle transmission rate control for cooperative active safety system,” *IEEE Trans. Intell. Transp. Syst.*, vol. 12, no. 3, Oct. 2010.
- [41] Y. P. Fallah, C. L. Huang, R. Sengupta, and H. Krishnan, “Analysis of information dissemination in vehicular ad-hoc networks with application

- to cooperative vehicle safety systems," *IEEE Trans. Veh. Technol.*, vol. 60, no. 1, Oct. 2010.
- [42] R. Stanica, E. Chaput, and A.-L. Beylot, "Reverse back-off mechanism for safety vehicular ad hoc networks," *Elsevier Ad Hoc Networks*, vol. 16, May 2014.
- [43] C. Song, "Performance analysis of the IEEE 802.11p multichannel MAC protocol in vehicular ad hoc networks," *MDPI Sensors*, vol. 17, 2017.
- [44] A. I. Abu-Khadrah, A. Zakaria, M. Othman, and M. S. Zin, "Enhance the performance of EDCA protocol by adapting contention window," *Springer Wireless Personal Communications*, vol. 96, no. 2, Sep. 2017.
- [45] R. Moraes, P. Portugal, F. Vasques, and R. F. Custodio, "Assessment of the IEEE 802.11e EDCA protocol limitations when dealing with real-time communication," *EURASIP J. Wirelss Commun. Netw.*, Dec. 2010.
- [46] S. Kim and Y. J. Cho, "Adaptive transmission opportunity scheme based on delay bound and network load in IEEE 802.11e wireless LANs," *J. Appl. Res. Technol.*, vol. 11, no. 4, Aug. 2013.
- [47] P. Patel and D. K. Lobiyal, "A simple but effective collision and error aware adaptive back-off mechanism to improve the performance of IEEE 802.11 DCF in error-prone environment," *Springer Wireless Pers. Commun.*, vol. 83, no. 2, Jul. 2015.
- [48] M. Karaca, S. Bastani, and B. Landfeldt, "Modifying backoff freezing mechanism to optimize dense IEEE 802.11 networks," *IEEE Trans. Veh. Technol.*, vol. 66, no. 10, Oct. 2017.
- [49] M. AlHubaishi, T. Alahdal, R. Alsaqour, A. Berqia, M. Abdelhaq, and O. Alsaqour, "Enhanced binary exponential backoff algorithm for fair channel access in the IEEE 802.11 medium access control protocol," *Int. J. Commun. Syst.*, vol. 27, no. 12, Dec. 2014.
- [50] N. O. Song, B. J. Kwak, J. Song, and M. Miller, "Enhancement of IEEE 802.11 distributed coordination function with exponential increase exponential decrease backoff algorithm," in *Proc. IEEE VTC 2003-Spring*.
- [51] K. Ashrafuzzaman and A. O. Fapojuwo, "Efficient and agile CSMA in capillary M2M communication networks," *IEEE Access*, vol. 6, Jan. 2018.
- [52] S. Kim, "Coexistence of wireless systems for spectrum sharing," *PhD Dissertation*, Virginia Tech, Jul. 2017.
- [53] T. Dessalgn and S. Kim, "Danger aware vehicular networking," in *Proc. IEEE SoutheastCon 2019*.
- [54] S. Kim and B. J. Kim, "Reinforcement learning for accident risk-adaptive V2X networking," *arXiv:2004.02379*, Apr. 2020.
- [55] S. Kim and C. Dietrich, "A novel method for evaluation of coexistence between DSRC and Wi-Fi at 5.9 GHz," in *Proc. IEEE Globecom 2018*.
- [56] D. Daley and D. Vere-Jones, *An Introduction to the Theory of Point Processes: Volume I: Elementary Theory and Methods*, Springer Probability and its Applications, Second edition, 2003.
- [57] S. N. Chiu, D. Stoyan, W. S. Kendall, and J. Mecke, *Stochastic Geometry and Its Applications*, pp. 3840 and 5354, Jun. 2013.
- [58] US Department of Transportation, "Speed concepts: informational guide," *Publication No. FHWA-SA-10-001*, pp. 17-19, Sep. 2009.
- [59] W. Manda, S. H. Steiner, R. J. MacKay, and A. R. Hilal, "Using telematics data to find risky driver behaviour," *Accident Analysis & Prevention*, Aug. 2019. [Online]. Available: <https://www.sciencedaily.com/releases/2019/08/190821082233.htm>
- [60] G. Bianchi, "Performance analysis of the IEEE 802.11 distributed coordination function," *IEEE J. Sel. Areas Commun.*, vol. 18, no. 3, Mar. 2000.
- [61] M. Haenggi, "On distances in uniformly random networks," *IEEE Trans. Inf. Theory*, vol. 51, no. 10, Oct. 2005.
- [62] IEEE, "IEEE 1609.4-2010, IEEE standard for wireless access in vehicular environments (WAVE)—multi-channel operation, Feb. 2011.